CERIC EXPERIMENTAL REPORT
Proposal number: 20227112
Title: Unraveling the De-/Lithiation Mechanism of different (Bismuth-doped) Niobium Oxides via *ex situ* and *operando* X-ray Absorption Spectroscopy

Proposer: Giovanni Orazio LEPORE

Beamline(s): LISA@ESRF

Shift: 18

Achievements: Within this experiment, *operando* X-ray absorption spectroscopy was conducted for both non-doped monoclinic and (Bi-doped) orthorhombic Nb_2O_5 in the 1st and 200th cycles at either Nb K-edge or Bi L_{III}-edge, complemented by *ex situ* measurements for electrodes after 200 cycles. Spectra at the Nb K-edge and Bi L_{III}-edge were collected in transmission mode, and simultaneously in fluorescence mode for the Bi L_{III}-edge. A preliminary analysis of the XANES indicates that: i) The local environment of monoclinic Nb_2O_5 between the 1st and 200th cycles is different. ii) The Nb K-edge for orthorhombic (Bi-doped) Nb_2O_5 exhibits an intense evolution in the local geometry in the first cycle. Nevertheless, its oxidation state reaches the initial state (Nb^{5+}) after a full cycle, which is in agreement with the *ex situ* XANES data. iii) The spectra at the Bi L_{III}-edge reveal a reduction from Bi^{3+} to metallic bismuth, and then further to Li_xBi. Upon delithiation, Bi was only partially reoxidized to its metallic form after the first full cycle. During the 200th cycle, the same behavior was observed, i.e., at 0.01 V, the Li_xBi alloy is formed and at 3.0 V, metallic Bi^0 was found, but with a bit low oxidation state.

_____ do not change anything above this line _____

1) Report

Graphite is still the anode material of choice for lithium-ion batteries (LIBs) due to its high theoretical capacity of around 370 mAh g^{-1} vs. Li^+/Li, low de-/lilthiation potential, enabling high specific energy at the full cell level. However, the slow kinetics of the lithium intercalation may lead to serious lithium plating during rapid charging, particularly at low temperatures.[1] For this reason, finding an alternative anode active material to enable fast charging while maintaining a high degree of safety is of utmost importance. Among the many possibilities, Nb_2O_5 attracted increasing attention recently, due to its promising performances in the voltage range of 0.01-3.0 V, similar to graphite. Research on Nb2O5 is also attracting a lot of attention owing to its rich structural chemistry. Different calcination temperatures can yield different Nb_2O_5 polymorphs, each exhibiting distinctive electrochemical behavior upon cycling. For instance, monoclinic Nb_2O_5 (H-Nb_2O_5) shows fast lithium diffusion through the tunnels within the octahedral blocks enclosed by shear planes.[2] Peculiarly, the initial structure remains unchanged upon dis-/charge in the voltage range from 0.01 V to 3.0 V, leading to a high reversible initial specific capacity of around 400 mAh g^{-1}, but it suffers from pronounced fading upon long-term cycling. A different polymorph, orthorhombic Nb_2O_5 (T-Nb_2O_5) can be synthesized when applying lower calcination temperatures, and shows a pronounced pseudo-capacitive behavior.[3] The initial phase transition from T-Nb_2O_5 to a NbO-type phase and further to monoclinic B-phase Nb_2O_5 in the initial cycle appears to contribute to good cycling stability and rate capability. Introducing bismuth as a dopant into the T-Nb_2O_5 host structure leads to an increase of the initial capacity up to about 450 mAh g^{-1} at 0.05 A g^{-1}, which decreases to around 300 mAh g^{-1} after 200 cycles at 0.2 A g^{-1}. In our previous experiment (CERIC 20217084), the *ex situ* XAS spectra for the 1st and 2nd cycles were collected, showing that the structures of both T-Nb_2O_5 and H-Nb_2O_5 develop in a very complex way upon cycling. However, the *ex situ* spectra do not provide real-time structural evolution during the whole de-/lithiation process. *Operando* XAS measurements, as performed herein, now filled this gap: the *operando* pouch cells comprised pristine electrodes and electrodes recovered after the 200 cycles to obtain data at different stages of the long-term cycling process. The pouch cells for the *operando* measurements were assembled in a dry room with a dew point below -70 °C. These cells were sealed and transported in a dry state to LISA@ESRF. Shortly before the experiment, a blister containing the electrolyte was opened to allow the electrolyte to wet the electrodes and separator. After that, the cell was connected to portable potentiostat Biologic VSP-150 for galvanostatic cycling. Considering that the cell configuration influences the overpotential and electrochemical performance, we compared each result with the *ex situ* samples at certain potentials to validate the *operando* data.

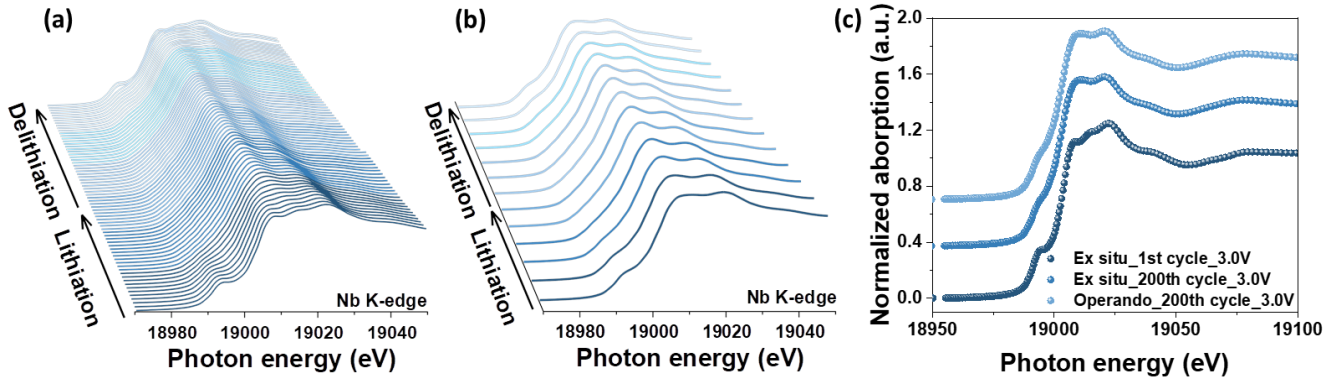

Figure 1. *(a-b) Operando Nb K-edge XANES spectra of H-Nb_2O_5 during the (a) 1st cycle and (b) 200th cycle. (c) Comparison of the ex situ spectra obtained for the recovered electrode at 3.0 V in the 1st and 200th cycle and the corresponding spectrum at 3.0 V obtained during the operando experiment.*

Figure 1a displays the XANES spectra of H-Nb_2O_5 at the Nb K-edge obtained during the *operando* experiment in the 1st cycle. From these data it is possible to detect a shift towards lower energies upon lithiation, followed by a restoration of the initial state upon delithiation. The evolution of the spectra during the 200th cycle (Fig.1b) looks similar as during the 1st cycle: the pre-edge was shifted towards lower energy upon lithiation, since the insertion of Li^+ results in a reduction of oxidation state of Nb. However, the comparison of the two cycles and the *ex situ* data reveal some minor differences, indicative of incremental structural changes occurring upon cycling (Figure 1c). Accordingly, the results provide a good explanation for the relatively high Coulombic efficiency in the first cycle and the gradual capacity upon cycling.

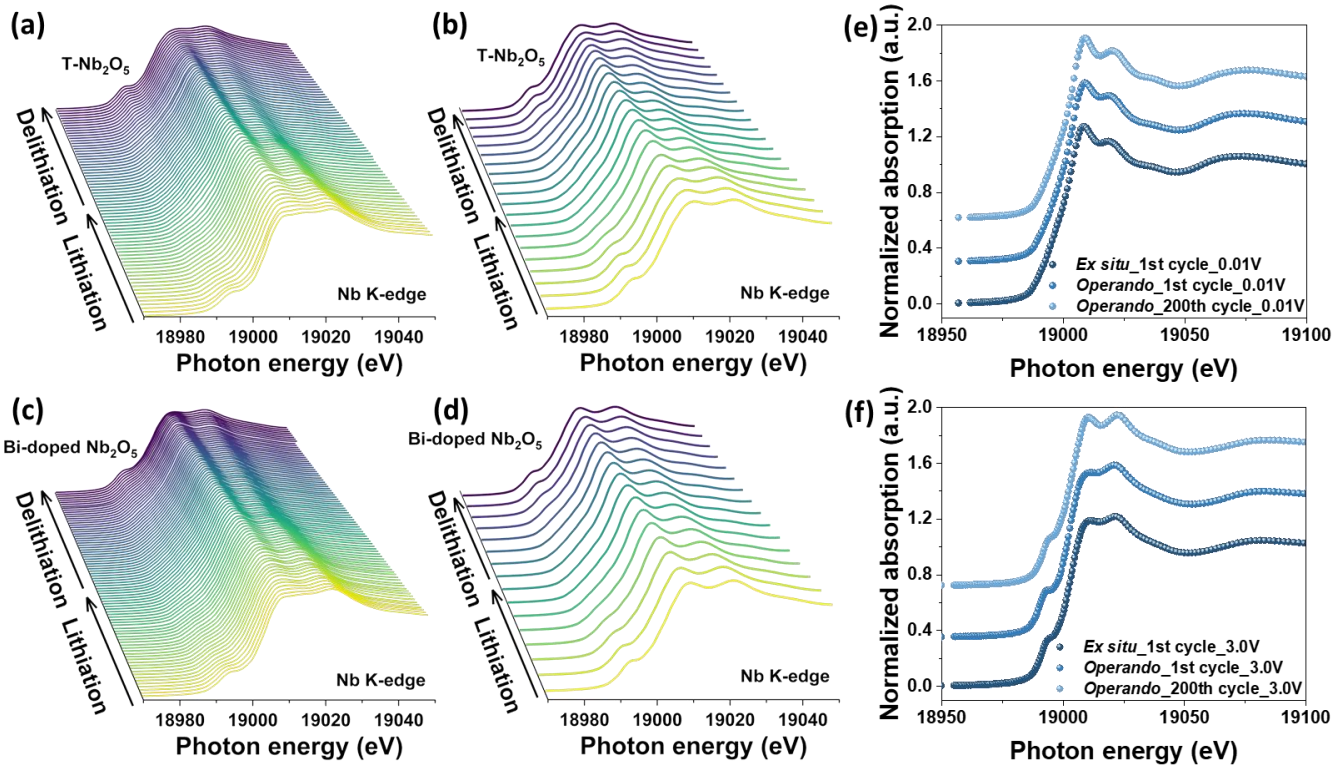

Figure 2. *(a-b) Operando Nb K-edge XANES spectra of T-Nb_2O_5 recorded during the (a) 1st cycle and (b) 200th cycle. (c-d) Operando Nb K-edge XANES spectra of Bi-doped Nb_2O_5 recorded during the (c) 1st cycle and (d) 200th cycle. (e) Comparison of the ex situ XANES spectra obtained for the recovered T-Nb_2O_5 electrode at 0.01 V in the 1st cycle and the corresponding spectra at 0.01 V obtained during the operando experiments in the 1st and 200th cycle. (f) Comparison of the ex situ XANES spectra obtained for the recovered T-Nb_2O_5 electrode at 3.0 V in the 1st cycle and the corresponding spectra at 3.0 V obtained during the operando experiments in the 1st and 200th cycle.*

In the case of (Bi-doped) Nb_2O_5, the overall evolution of the Nb K-edge spectra displayed a nearly-consistent trend. The first cycle exhibits an irreversible structural change, while the subsequent cycles maintain a similar overall structure with minor changes, as displayed in **Fig. 3**. Regarding the spectra collected at the Bi L_{III}-edge, the bismuth dopant was gradually reduced to metallic bismuth and further to lithium bismuth alloy when the fully reacted to Li_xBi at 0.01 V, as the pre-edge and L_{III}-edge are situated between the calculated monoclinic Li_3Bi and calculated/experimental Bi metal. Upon reoxidation, the bismuth species returned to metallic bismuth at 3.0 V. A lower shift in the edge position was observed between 1st and 200th cycle, indicating that the bismuth was involved in an irreversible electrochemical reaction, which leads to a lower specific capacity after a few cycles. The results are displayed in **Fig.4**.

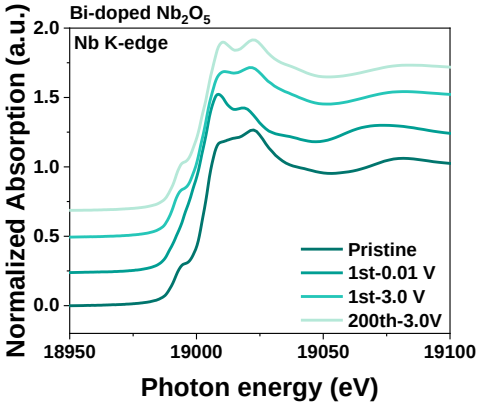

Figure 3. *The Nb K-edge spectra of the selected Bi-doped Nb_2O_5 samples from operando XANES measurements for comparison.*

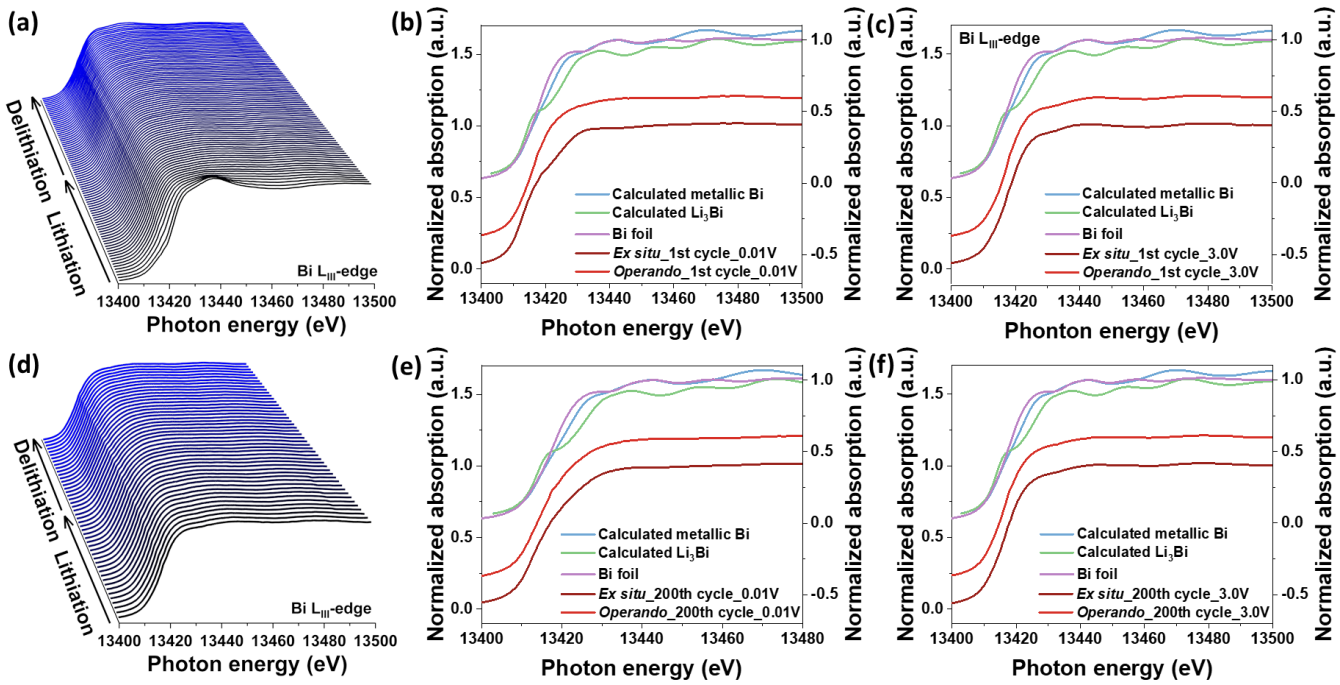

Figure 4. *(a) Operando Bi L_{III}-edge XANES spectra and (b,c) comparison of the operando and ex situ spectra of Bi-doped Nb_2O_5 (b) at 0.01 V, and (c) at 3.0 V recorded during the 1st cycle. (d) Operando Bi L_{III}-edge XANES spectra and (e,f) comparison of the operando and ex situ spectra of Bi-doped Nb_2O_5 (e) at 0.01 V and (f) at 3.0 V recorded during the 200th cycle.*

In summary, the preliminary analysis of the *operando* results is generally in line with the *ex situ* experiments. Further quantitative investigation and in-depth EXAFS analysis will advance the mechanistic understanding of this class of fast-charging anodes and facilitate further research in this area. In addition, we would like to mention that we are as always very satisfied with the high-quality spectra collected at this beamline and the professionalism of the beamline staff throughout the experiment.

2) Reference

[1] J. Asenbauer, T. Eisenmann, M. Kuenzel, A. Kazzazi, Z. Chen, D. Bresser, *Sustain. Energy Fuels* **2020**, *4*, 5387–5416.

[2] K. J. Griffith, I. D. Seymour, M. A. Hope, M. M. Butala, L. K. Lamontagne, M. B. Preefer, C. P. Koçer, G. Henkelman, A. J. Morris, M. J. Cliffe, S. E. Dutton, C. P. Grey, *J. Am. Chem. Soc.* **2019**, *141*, 16706–16725.

[3] K. J. Griffith, A. C. Forse, J. M. Griffin, C. P. Grey, *J. Am. Chem. Soc.* **2016**, *138*, 8888–8899.